# Computational fluid dynamics analysis of diffuser performance in gas-powered jet pumps

**R. S. Neve**
Thermo-Fluids Engineering Research Centre, Department of Mechanical Engineering and Aeronautics, City University, London UK

Jet pump diffuser performance is analyzed, both in terms of past experimental work dealing with the high inlet flow distortions involved and in the sense that this problem is amenable to predictive investigation by computational fluid dynamics techniques. In these highly nonuniform flow conditions, diffusers are seen to justify their inclusion in a jet pump design, for regaining static pressure downstream of the vacuum chamber, even though their performance in effectiveness terms is lowered by about two thirds at high inlet flow distortion levels. A satisfactory correlation has been found between outlet and inlet conditions and diffuser area ratio, extending well beyond past experimental published results for diffuser geometry and distorted inlet flows.

**Keywords**: diffusers; jet pumps; ejectors; distorted flow; computational fluid dynamics

## Introduction

Jet pumps or ejectors are concerned with using a jet of primary fluid to induce a peripheral secondary flow, often against a substantial back pressure. The induction process produces a partial vacuum in the secondary flow inlet so this fluid is subject to a rapid repressurization to the jet pump exit section value, and a diffuser is normally found useful in producing the change from a low-pressure, fast-moving flow to a higher pressure, slower fluid at outlet (Engineering Sciences Data Unit 1988a, 1988b) (Figure 1). The diffuser is found useful even in liquid-gas multiphase flows (Neve 1988, 1991, Owen et al. 1992), although its pressure recovery performance suffers increasingly as void fraction rises above about 20 percent, and there is genuine doubt whether the diffuser is of any use at all at void fractions above 60 percent. At the extreme case of *very* high void fraction (spray in a duct), however, the diffuser again becomes valuable.

The essential fact here is that diffusers perform best with a uniform inlet velocity profile of a single-phase flow and progressively less well as nonuniformities increase. Unfortunately, many industrial applications require diffusers to be positioned downstream of bends, blockages, valves, turbomachines, and so forth, leading to poorer performance. The jet pump must be considered at least as bad as any of the cases described earlier, with, at its worst, a jet being fired into a diffuser inlet after only a short length of mixing tube. The worst case would be where a jet pump was maintaining a partial vacuum in a nearby region with virtually no flow rate; the ratio of secondary to primary flows $Q_s/Q_p$ is then effectively 0.

The designer has a delicate choice to make in specifying a mixing tube length: a short one involves lower wall skin friction losses but a higher inlet velocity distortion factor. A long diffuser is definitely not the answer to this problem because not only does that involve even more wall friction losses, but distortion factors nearly always increase with downstream travel in expanding ducts (Neve and Wirasinghe 1978; Priest 1975; Sprenger 1962). To these performance impediments must be added the complications that increased noise and mechanical vibrations are always associated with the transient flow changes in stalled diffusers.

This article addresses the problem of how badly diffuser performance is affected by highly distorted inlet flows and reports the results of a computational fluid dynamics (CFD) analysis of the problem, backed up by published experimental data, where these are applicable.

Address reprint requests to Professor Neve at the Thermo-Fluids Engineering Research Centre, Department of Mechanical Engineering and Aeronautics, City University, London, EC1V 0HB, UK.

Received 14 December 1992; accepted 21 June 1993



## Diffuser performance

The most fundamental definition of diffuser efficiency $\eta$ was set down by Patterson (1938). This is essentially the ratio of power transformed (a "flow work" term) to the difference in kinetic energies between inlet and outlet. In incompressible flow, this is

$$\eta = \frac{\int_{A_2} pu\,dA - \int_{A_1} pu\,dA}{\int_{A_1} \frac{1}{2}\rho V^2 u\,dA - \int_{A_2} \frac{1}{2}\rho V^2 u\,dA} \quad (1)$$

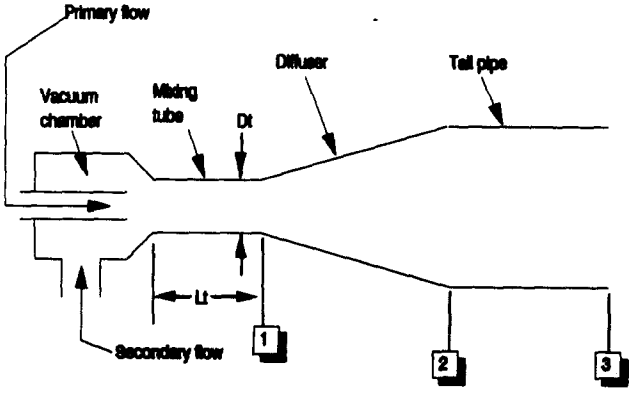


*Figure 1* Basic jet pump arrangement

where $V$ is the resultant velocity (in three dimensions) in the duct, and $u$ is its axial component. The summation process implied by the integral signs is nearly always tedious and time-consuming to carry out, but in many cases such rigor is not required. For example, uniformity of pressure and velocity over a cross section leads to much cancellation, and Equation 1 reduces to that for pressure recovery coefficient, $C_p$.

$$C_p = \frac{p_2 - p_1}{\frac{1}{2}\rho\bar{u}_1^2} \tag{2}$$

where $\bar{u}_1$ is the space-mean value of $u$ over the diffuser inlet section.

The Engineering Sciences Data Unit (1973, 1976) data sheets dealing with diffusers include not only copious references to this subject but also graphical data enabling performance to be estimated for diffusers subject to uniform or slightly distorted inflows. Care is needed, however, for markedly nonuniform inflows because not only will $p_1$ be artificially depressed by the high peak inlet velocity, but the denominator of Equation 2 is based on the space-mean inlet velocity, which could be much lower than the peak value. Pressure recovery coefficient can therefore rise significantly above unity in these cases.

It has often been found better to use the kinetic energy factor $\alpha$ as a measure of distortion. This is defined as the ratio of true kinetic energy to the value based on the space-mean velocity and for incompressible flow would be

$$\alpha = \int_A u^3 dA/A\bar{u}^3 \tag{3}$$

Then a value of $C_p$ for an ideal diffusion process can be defined by

$$C_{pi} = \frac{\alpha_1(\frac{1}{2}\rho\bar{u}_1^2) - \alpha_2(\frac{1}{2}\rho\bar{u}_2^2)}{\frac{1}{2}\rho\bar{u}_1^2}$$

$$= \alpha_1 - \alpha_2/(AR)^2 \tag{4}$$

In uniform flow, $\alpha$ would have the value 1.0 but in any other case would be greater. For flows where a boundary layer constitutes the only nonuniformity, $\alpha$ can be as low as 1.04 but diffuser outlet values $\alpha_2$ can be as high as 4 for grossly distorted inflows (Neve and Wirasinghe 1978; Priest 1975). In particular, Neve and Wirasinghe have shown how $\alpha$ climbs from an entry value of 1.1 to exit values of about 2.5, 3, and 4 for diffusers of total cone angle 10°, 20°, and 30°, respectively.

The diffuser's so-called effectiveness can then be defined as the ratio of the measured $C_p$ to that for the ideal diffusion case.

$$\bar{\eta} = C_p/C_{pi} \tag{5}$$

In practice, even the calculation of $\alpha$ can be a tedious process, and researchers have therefore often resorted to simpler, but justifiable, means of defining nonuniformity. Sovran and Klomp (1965) used an effective area fraction $E$ ($=\bar{u}/u_{max}$), a parameter easily calculated because $\bar{u}$ is the volumetric flow rate divided by the cross-sectional area. They justified this approach by showing a good correlation between $E_1$, $E_2$, and diffuser area ratio $AR$, but their inlet profiles did not extend beyond the fully developed pipe flow type ($E = 0.84$).

Tyler and Williamson (1967) set out to extend this approach to higher distortion levels and attempted to find correlations between outlet and inlet values of several parameters including two based on E: the blockage $B(= 1 - E)$ and a distortion factor $DF$ ( $= 1/E$). From the equations linking inlet and outlet conditions, Tyler and Williamson derived a nominal outlet distortion factor $DF_{2n}$

$$DF_{2n} = (AR)[DF_1^2 - C_p]^{1/2} \tag{6}$$

and then found a good correlation for outlet distortion in terms of inlet distortion and $AR$ for diffuser geometries not too far removed from the ideal $2\theta = 7°$ suggested in most data sheets. Using data from Cockrell and Markland (1963), Winternitz and Ramsay (1957) and Sprenger (1962), involving area ratios from 1.5 to 4, they justify the following relationship for distortions greater than fully developed pipe flows ($B_1 > 0.16$, $DF_1 > 1.19$):

$$B_{2n} = 1.044 - 1.13(1 - B_1)/(AR)^{0.69} \tag{7}$$

If this type of approach could be used for very high inlet $DF$ values, as in jet pumps, then a $C_p$ value could be obtained from Equation 6, and designers could better predict the performance of projected jet pumps for specified duty. This project therefore involved setting up CFD models of jet pumps and, by implication, mixing tube/diffuser/tail pipe combinations to investigate the relationship between outlet conditions and

## Notation

| | |
|---|---|
| $A$ | Area |
| $AR$ | Area ratio $A_2/A_1$ |
| $b$ | Mixing tube area ratio $A_j/A_t$ |
| $B$ | Blockage ($=1 - E$) |
| $C_p$ | Pressure recovery coefficient (Equation 2) |
| $D$ | Diameter |
| $dA$ | Increment of area |
| $DF$ | Distortion factor $u_{max}/\bar{u}$ |
| $E$ | Effective area fraction $\bar{u}/u_{max}$ ($=1/DF$) |
| $f$ | Friction factor $2\tau_w/\rho\bar{u}^2$ |
| $k$ | Kinetic energy per unit mass of turbulent fluctuations |
| $L$ | Length |
| $p$ | Static pressure |
| $Q$ | Volumetric flow rate |
| Re | Reynolds number $\bar{u}D\rho/\mu$ |
| $u$ | Axial component of resultant velocity (time mean) |
| $V$ | Resultant velocity ($=u$ if there are no radial or tangential components) |

*Greek letters*

| | |
|---|---|
| $\alpha$ | Kinetic energy shape factor (Equation 3) |
| $\varepsilon$ | Turbulence dissipation rate |
| $\mu$ | Dynamic viscosity |
| $\eta$ | Diffuser efficiency (Equation 1) |
| $\bar{\eta}$ | Diffuser effectiveness (Equation 5) |
| $\rho$ | Fluid density |
| $\theta$ | Diffuser cone half-angle |
| $\tau$ | Shear stress |

*Subscripts*

| | |
|---|---|
| 1 | Diffuser inlet section |
| 2 | Diffuser outlet section |
| 3 | Tail pipe outlet section |
| j | Jet |
| max | Maximum value |
| p | Primary fluid |
| s | Secondary fluid |
| t | Mixing tube |
| w | Wall value |

An overbar (except for $\bar{\eta}$) indicates a space-mean value over a cross section

highly distorted inflows in an attempt to correlate $DF_{2n}$, $DF_1$, and $AR$ over a very wide range of $DF_1$ values, comparison being made with empirical data, where possible, to validate the computational predictions.

## Computer modeling procedure

Version 1.6 of the PHOENICS CFD package, marketed by CHAM Ltd. of Wimbledon, was used in this project. This is a finite volume technique, in the present case using a body-fitted coordinates method for grid generation. The $k-\varepsilon$ option was used for turbulence modeling because this has found wide acceptance and seems particularly applicable to problems involving moderate to high Reynolds numbers, especially those involving separated or reattaching flows. $k$ is the kinetic energy per unit mass of the turbulence fluctuations and was set for an inlet relative turbulence intensity of 10 percent. $\varepsilon$ is the turbulence dissipation rate and is proportional to $k^{3/2}$ divided by a characteristic length (Prandtl-Kolmogorov). This gives a kinematic eddy viscosity $v_t$ of $C_\mu k^2/\varepsilon$, where $C_\mu$ varies somewhat with application but was here given the usual value of 0.09, the PHOENICS default setting.

Other choices set within the PHOENICS program were that a "whole field" solution was required, because of the recirculatory nature of the flows involved here, and the diffusion terms were suppressed in favor of the convective ones to speed up the computation process. A linear relaxation factor of 0.3 was set for the pressure field, as recommended by CHAM for body-fitted coordinate cases, and a "FALSDT" value of 1 ms, related to typical residence times, for the remaining variables. Wall friction was set using a log law type of profile for the turbulent boundary layers involved.

The question of grid fineness is always a contentious one because a choice must be made between the advantages of finer grids giving greater accuracy of prediction and their disadvantages of longer computer run times. Finer grids also involve larger storage requirements for results and the analysis of such a large body of numbers can sometimes be daunting. It is normally essential to ensure sufficient fineness in the direction in which parameters are changing most rapidly, in this case the radial one. A grid to model a jet pump and having 35 cells in the axial direction was therefore set up and tested with various numbers of cells in the radial direction. Only one cell width (a circular sector) was needed in the tangential direction because the problem is axisymmetric. The time taken for each case, and the pressure and axial velocity in a specified cell were monitored to investigate cell fineness effects.

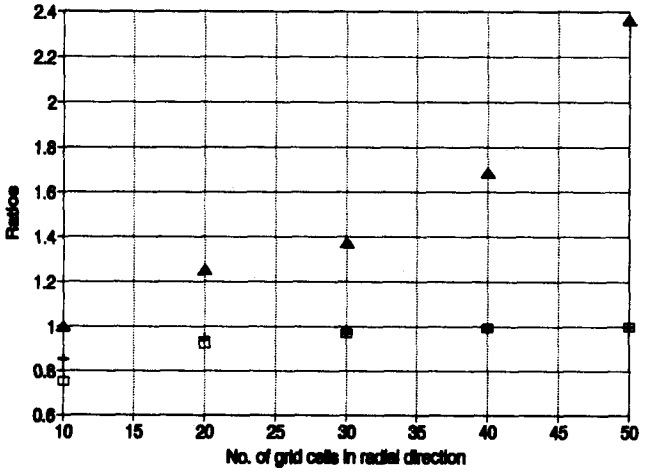


*Figure 2* Effect of grid fineness on results: ▲ Run time ratio ($T/T_{10}$); + Pressure ($p/p_{50}$); □ Velocity ($u/u_{50}$)

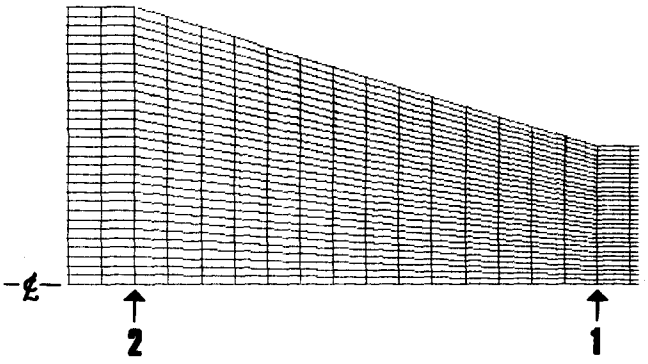


*Figure 3* PHOENICS mesh for a 30 (radial) by 14 (axial) diffuser

Figure 2 shows how the parameters compare for cases of 10 to 50 radial cells. Computer run time starts to increase steeply for more than 40 cells, and pressure and velocity are not given with very much greater predictive accuracy if more than 30 cells are used. Results would seem to be within about 2 percent of the 50-cell case if only 30 cells are involved so a 35 (axial) × 30 (radial) × 1 (tangential) cell grid was used for most of the cases presented here. Figure 3 shows a PHOENICS printout of a diffuser of total cone angle 40° and with 30 equispaced cells per radius. The number of cells in the axial direction assigned to the diffuser and its entry and tail pipes can be varied as required, as can their relative lengths, but in all cases the full extent of the mixing tube was modeled.

Versatility is also required in the radial direction. With reference to Figure 1, designers must choose a jet to mixing tube area ratio b to suit their application. A slim jet in a wide tube (low b) draws in more secondary fluid than a wide jet but cannot withstand such high back pressures as the wide one. Values of b from about 0.25 to 0.5 are common, and these have therefore been used as range limits in this project. The value of b is controlled by the radial proportion of cells at the inlet station that carries primary fluid, and this is easily set up in the PHOENICS syntax. The axial velocity set for these inlet cells was 100 m/s, low enough to avoid compressibility problems but high enough to ensure realistic Reynolds numbers. The speed of the secondary fluid at the inlet station was chosen to give various $Q_s/Q_p$ ratios from zero to a value ensuring a near-uniform diffuser inlet flow, that is, the only nonuniformities were in the boundary layers.

Large variations in distortion factor $DF_1$ were achieved by varying the mixing tube length $L_t/D_t$ over a wide range from 0 to about 12. Diffuser area ratios of 2, 4, and 5.6 were used and total cone angles of 7°, 10°, 15°, and 20°. This extension to values well above the empirically ideal 7° to 8° reflected the fact that designers often use wider angles where axial space is at a premium. Atmospheric pressure was set as a boundary condition across the tail pipe exit, although the absolute value was unimportant (in incompressible flow) because the program deals in pressure differences.

The PHOENICS program solves by iteration over a slab of cells perpendicular to the bulk flow direction and then sweeps downstream to subsequent slabs. Convergence is therefore achieved by making sufficient sweeps to minimize the parameter residuals; 200 such sweeps were made in each of the computer runs in this project. On a Sun Sparcstation, this took just over 7 min of run time.

## Discussion of CFD results

### Axial pressure distribution in jet pumps

Initial computational runs were carried out for jet pumps with conventional 7° diffusers and b ratios of 0.3, 0.4, and 0.5 but with artificially long mixing tubes so that the axial pressure distribution could be studied. No secondary flow was added in these cases so the distortion factor $DF$ has a very high value at inlet to the mixing tube. Figure 4 shows that static pressure is regained from its minimum value in the vacuum chamber but then lost steadily in the mixing tube, because of wall friction. The $AR = 5.6$ diffuser appears effective in returning the flow to atmospheric pressure at the tail pipe exit, but it is also clear that diffusion is not quite complete at diffuser exit, so the tail pipe has a part to play in the diffusion process.

The pressure loss gradient in the mixing tube appears to be a function of $b$, but it should be remembered that the space-mean velocity is different in each case. For $b = 0.5$, this would be 50 m/s, and a calculation using Darcy's equation for the pressure loss in this case (using $f = 0.079/\mathrm{Re}^{0.25}$) would give $\Delta p/(\frac{1}{2}\rho\bar{u}^2) = 0.225$. For the $b = 0.3$ ($\bar{u} = 30$ m/s) case, this would be 0.256. The Reynolds numbers for these two cases (based on $\bar{u}$) were about $7.2 \times 10^4$ and $4.3 \times 10^4$. The normalized pressure plot of Figure 5 shows that these are almost exactly the mixing tube pressure drops predicted by the PHOENICS program, giving confidence in subsequent results.

Clearly these mixing tubes, having $L_t/D_t \simeq 12$, were too long because the static pressure drop is unacceptably large, but this, once again, shows the designer's dilemma: a long tube minimizes the worst effects of inlet distortions but involves a high penalty in pressure loss terms. The diffusers in each case give a pressure recovery, with the tail pipes, of about 0.63; this value should be compared with 0.75 quoted by McDonald and Fox (1966) and 0.76 by the Engineering Sciences Data Unit (1973, 1976) for *uniform* inlet flow.

### Distortion factor and mixing tube length

A set of runs was undertaken to predict how $DF_1$ would change with mixing tube length; the results are shown in Figure 6 and refer to the case of $b = 0.25$ and no secondary flow. The initial value is therefore 4, but this parameter subsequently falls rapidly, once the mixing process is established, and would clearly reach its fully developed pipe flow value of $DF = 1.19$ after about 3 tube diameters. Mixing tubes longer than this are

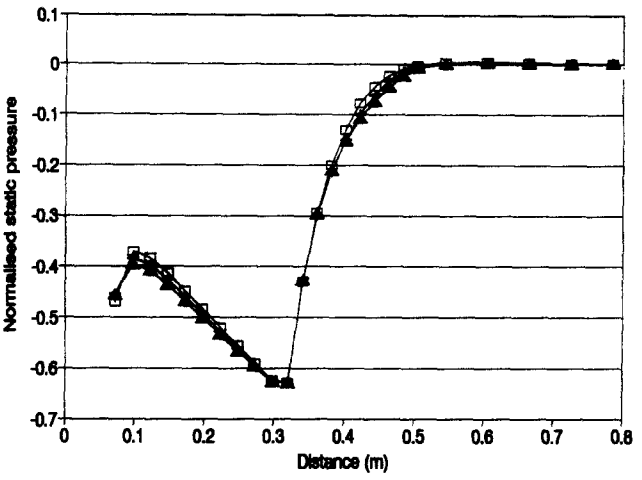


*Figure 5* Normalized static pressure distribution (data as for Figure 4)

therefore pointless, except in liquid jet cases with gas secondary flows (Neve 1988), where the jet needs to disintegrate before any serious gas ingestion can occur.

### Distortion factor and diffuser performance

Figure 7 shows how gas ingestion affects $DF_1$ and how that, in turn, affects $C_p$. This is for a 15°, $AR = 2$ diffuser having $b = 0.25$ and $L_t/D_t = 1.5$. As the secondary flow ratio $Q_s/Q_p$ rises from 0 to 3 (i.e., from the worst possible case to approximately uniform flow), $DF$ falls from 3 (its value after 1.5 diameters of mixing tube) to about unity, as required. Over the same range, $C_p$ falls from a value well above unity, as predicted, to 0.48. This last figure agrees closely with the empirical value of 0.46 given by the Engineering Sciences Data Unit (1973, 1976) for uniform inflow.

Efficiencies, conversely, might be expected to rise with increasing $Q_s/Q_p$ because the introduction of secondary flow would ventilate (pressurize) the separated region between the upstream end of the primary jet and the nearby mixing tube wall. The efficiencies $\eta_2$ and $\eta_3$, defined in Equation 1, have been calculated using the PHOENICS output files' pressures and velocities at diffuser and tail pipe exits, respectively, a

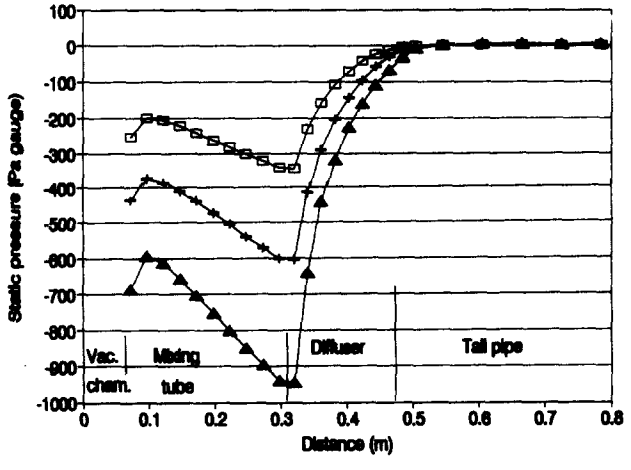


*Figure 4* Predicted static pressure distribution in jet pumps: AR = 5.6; $2\theta = 7$ deg.; $D_t = 21.5$ mm; $u_j = 100$ m/s; □ b = 0.3; + 0.4; ▲0.5

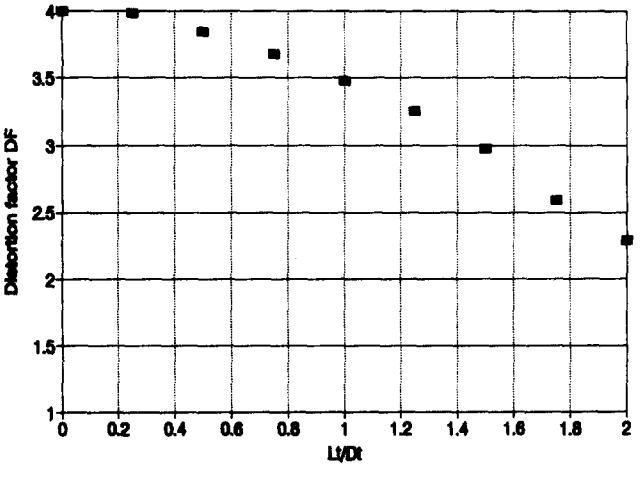


*Figure 6* Effect of mixing tube length on inlet distortion factor: b = 0.25; $Q_s/Q_p = 0$; $D_t = 200$ mm; $u_j = 100$ m/s

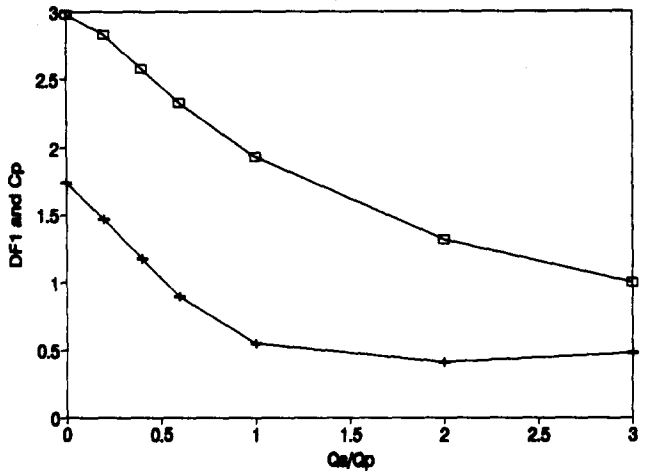


*Figure 7* Effect of secondary flow ratio on $C_p$ and $DF_1$: b = 0.25; $L_t/D_t = 1.5$; AR = 2; $2\theta = 15$ deg; □ $DF_1$; + $C_p$

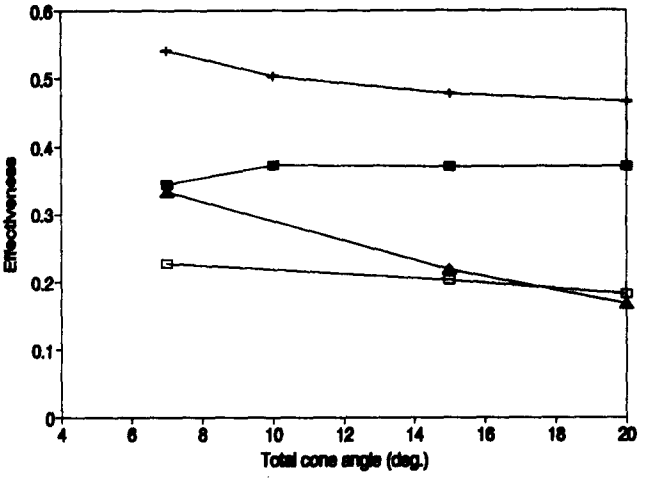


*Figure 9* Effect of diffuser cone angle on effectiveness: ■ $DF_1 = 3.6$; AR = 4; + $DF_1 = 1.6$; AR = 4; ▲ $DF_1 = 3.9$; AR = 2; □ $DF_1 = 3$; AR = 2

process rendered considerably easier using spreadsheet techniques. It seems remarkable that these parameters actually decline (Figure 8) as secondary flow is introduced but then rise as $DF_1$ falls from 2 to 1 ($Q_a/Q_p$ rising from 1 to 3), finishing at values of $\eta_2 = 0.734$ and $\eta_3 = 0.767$. It may be that this initial drop in efficiency is the result of the ventilation process, mentioned earlier, causing a marked change in turbulence properties in this area. A reduction in turbulent mixing rates would certainly hinder the process of jet reattachment to the wall by what is generally regarded as Coanda effect, in this case an axisymmetric one. The ability of a flow to attach to a nearby offset wall has been demonstrated many times in the literature generated by fluidics research in the 1960s and 1970s, but Ferrett, Lampard, and Duggins (1972) have reported cases of diffusers of cone angles up to 20° producing improved pressure recoveries using a truncation method; that is, the cone is shorter, but the flow is subject to a sudden enlargement into a tailpipe of greater diameter. This is recommended, however, only for cases in which axial length is at a premium. Improvements are also reported by Migay (1963) and Stull (1975) using diffusers with ribbed walls, the diffuser flow reattaching to the next step corner after separating from the previous one. The physical processes in all these various cases would seem to be of the same nature.

Diffuser effectiveness $\bar{\eta}$, defined by Equation 5, is predicted to have very low values at low secondary flow ratios but then to climb to 0.639 for uniform flow. In this case, an experimental value is available for comparison: McDonald and Fox (1966) give 0.65 for $2\theta = 15°$ and $AR = 2$.

The influence of diffuser cone angle on effectiveness is shown in Figure 9. For an area ratio of 4, a lower inlet DF value (longer mixing tube) gives a higher $\bar{\eta}$, as expected, but higher cone angles seem to produce a slight improvement for the higher $DF$ case. For the $AR = 2$ diffusers, the higher distortion case appears to give a higher $\bar{\eta}$ for a 7° diffuser, but $DF$ has little effect at greater cone angles. These inconsistencies are not easy to explain but may indicate that high distortion factors produce separated flows, even in 7° diffusers and therefore that cone angle, certainly up to 20°, has little importance.

Continuing with 15° diffusers, Figure 10 shows how $C_p$ is affected by inlet distortion for three different area ratios. For uniform flow ($DF_1 = 1$), the $C_p$ prediction of 0.48 for $AR = 2$ has already been compared with the ESDU value of 0.46; the $AR = 4$ prediction of 0.52 compares slightly less well with the experimental figures of 0.55 from McDonald and Fox and 0.58 from ESDU. The rest of the figure shows how markedly $C_p$ increases above unity, for reasons given earlier, as $DF_1$ climbs to about 4, irrespective of area ratio. Effectiveness, conversely,

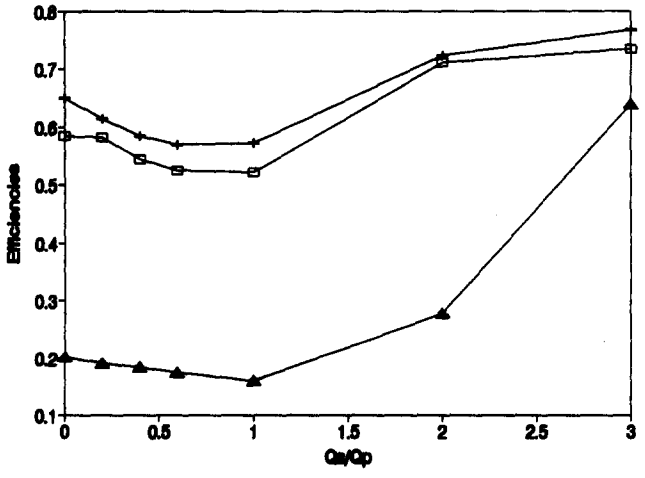


*Figure 8* Diffuser efficiencies and effectiveness (data as for Figure 7): □ $\eta_2$; + $\eta_3$; ▲ Effectiveness [Equation (5)]

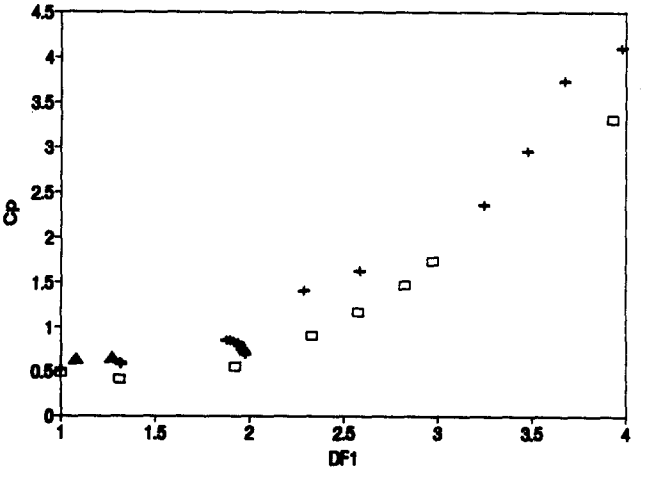


*Figure 10* Effect of distortion factor on $C_p$ ($2\theta = 15$ degrees): □ AR = 2; + 4; ▲ 5.6

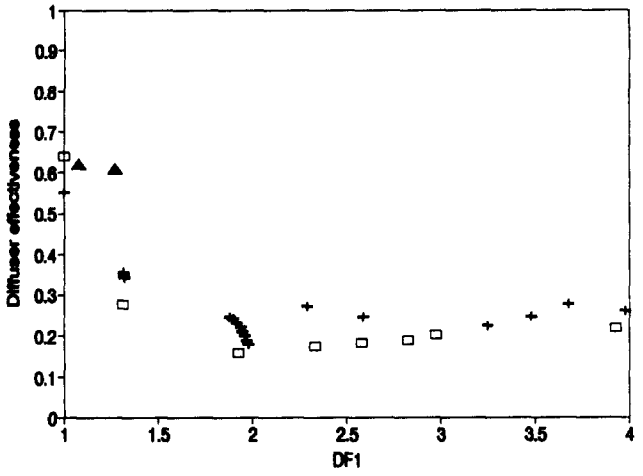


*Figure 11* Effect of distortion on diffuser effectiveness (data as for Figure 10)

falls fairly rapidly with $DF_1$ to about a third of its uniform flow value, once again irrespective of area ratio (Figure 11).

## Correlation of inlet and outlet parameters

It was the stated goal of Sovran and Klomp (1965) and Tyler and Williamson (1967) to determine a reliable correlation between inlet and outlet distortion parameters and diffuser area ratio. The former obtained such a relationship for inlet distortions no worse than fully developed pipe flow; the latter extended this to higher $DF$ values. The present work has extended distortion factors still further, to about 4, and comparison with Tyler and Williamson's results is therefore required.

Figure 12 shows how the nominal $DF_2$ value (Equation 6) varies with $DF_1$; clearly, area ratio is an associated variable. If $DF_{2n}$ is represented in its $B_{2n}$ form ($B = 1 - \{1/DF\}$), the results of Figure 12 can be compared with the "best fit" results of Tyler and Williamson (Equation 7) for each given area ratio; these are shown in Figure 13 where the lines represent the values of Equation 7 for the area ratios concerned. Agreement is seen to be fairly close, particularly at the high distortion end of the data range.

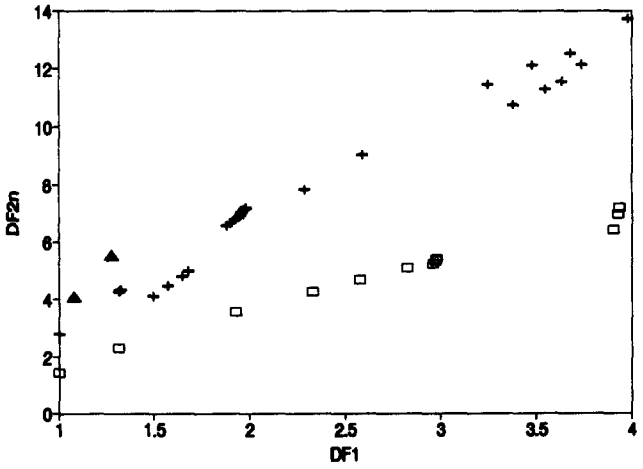


*Figure 12* Effect of inlet distortion on nominal outlet distortion: □ AR = 2; + 4; ▲ 5.6

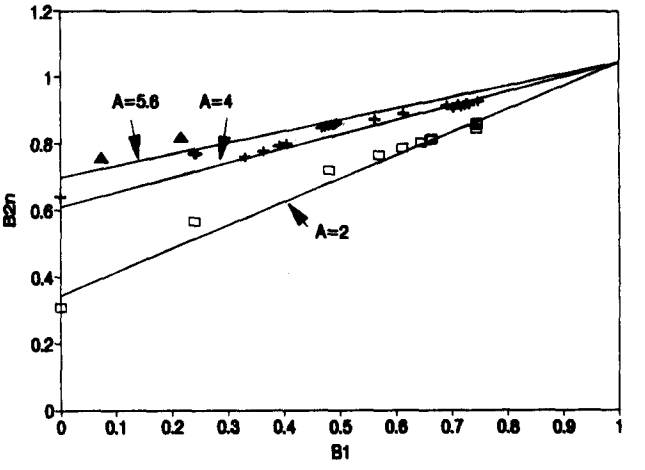


*Figure 13* Nominal outlet blockage vs. inlet blockage. Comparison of PHOENICS predictions ($7 < 2\theta < 20$ degrees) with Tyler and Williamson's correlation: □ AR = 2; + 4; ▲ 5.6

Data analysis shows, however, that the current results can be correlated more straightforwardly using 0.83 as the power of area ratio, rather than the 0.69 used by Tyler and Williamson, and $DF_{2n}$ divided by that quantity then correlates well with $DF_1$ (Figure 14). A data regression analysis shows the best fit straight line for the points in Figure 14 to be given by

$$DF_{2n}/(AR)^{0.83} = 1.035(DF_1) \quad (8)$$

The $R^2$ value for the straight line fit is 0.978. A curve fit involving second and third powers of $DF_1$ is not really warranted by the scatter involved; $R^2$ increases to only 0.981 for the quadratic and to 0.982 for the cubic.

## Contour plots from the computational results

The remaining four figures in this article show some of the graphical output from the PHOENICS runs, in these cases for a 15°, $AR = 4$ diffuser with $b = 0.25$, $L_t/D_t = 1.5$ and no secondary flow.

Predicted static pressure contours can be seen in Figure 15. A pressure of 2.71 kPa.vac. is generated close to the point where the primary jet enters the mixing area, and the tube is seen to

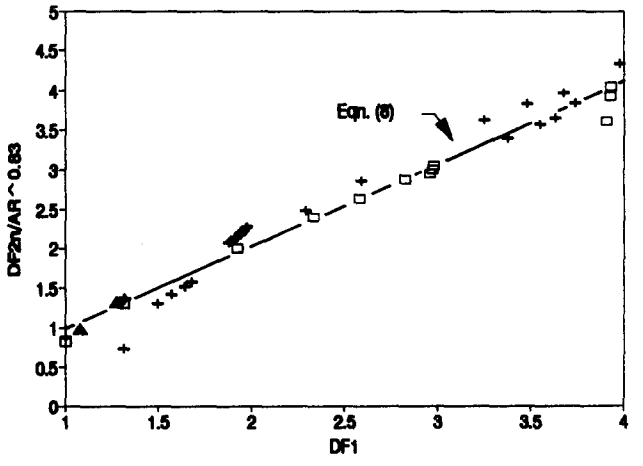


*Figure 14* Correlation of nominal outlet distortion function with inlet distortion (all diffusers): □ AR = 2; + 4; ▲ 5.6

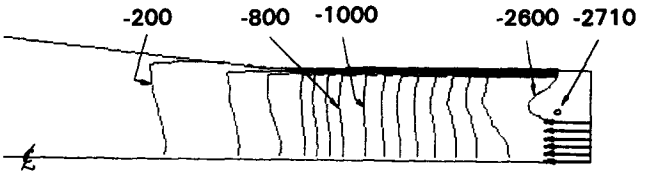


*Figure 15* Predicted pressure contours in the diffuser entry region. Figures are in Pa. gauge

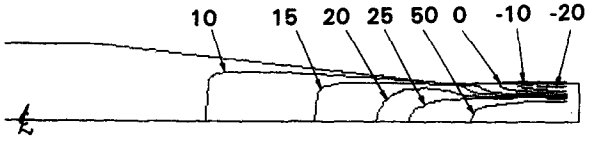


*Figure 16* Contours of axial velocity in the mixing tube and diffuser. Figures are in m/s

be very effective at raising this to above 1 kPa.vac. before the flow enters the diffuser. It is also clear from the contours that near the diffuser and mixing tube entry sections, static pressure is higher on the centerline than at the wall, an indication of the streamline curvature hereabouts.

The axial velocity contours are shown in Figure 16, which backs up Figure 15 in suggesting the presence of a reattachment vortex, with reversed flow velocities of at least 20 m/s. The 10 and 20 m/s contours in the diffuser show the extent of the boundary layers or separated regions next to the walls. The mean speed in the tail pipe will have been 6.25 m/s.

One advantage of using computational techniques is that variables can be calculated and inspected, which would otherwise be extremely difficult to measure experimentally. Figures 17 and 18 show, respectively, the $k$ and $\varepsilon$ contours for the near-jet regions. $k$ is the kinetic energy per unit mass of the turbulent fluctuating components and $\varepsilon$ the dissipation rate. Not surprisingly, both peak in the area of maximum shearing rate, between the emerging jet and the region under partial vacuum. In fact, the contours are very similar, in shape though not in numerical value.

## Conclusion

Despite the very considerable nonuniformities of inlet flow involved, the diffusers in jet pumps are predicted still to be necessary and useful for static pressure retrieval in single-phase devices. Comparison with published experimental data gives confidence in these CFD predictions.

Although pressure recovery coefficients for the diffusers were shown to increase markedly with increased inlet distortion factor, this was simply due to the way in which $C_p$ is defined. Diffuser effectiveness, a more realistic measure of performance, was shown to fall, for increasing inlet distortions, to about a third of its uniform flow value.

Mixing tubes longer than about 3 diameters are shown to be pointless, for single-phase flow, because the velocity profile has often smoothed itself to a fully developed pipe flow value by then, and greater pipe length simply involves more pressure losses. A designer could then use Figure 14 or Equation 8 to

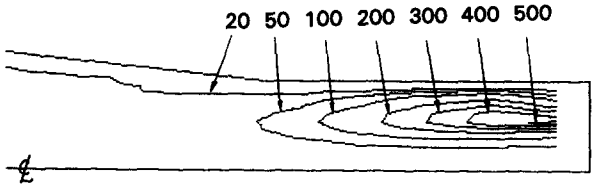


*Figure 17* Contours of k in the mixing region. Figures are in $m^2/s^2$

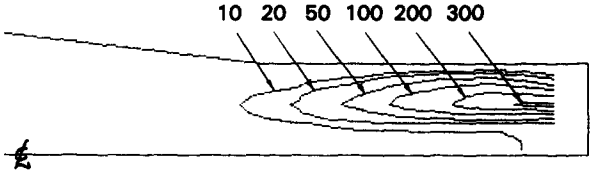


*Figure 18* Contours of $\varepsilon$ in the mixing region. Figures are in $(10^3 \times m^2/s^3)$

obtain a $DF_{2n}$ value for use in Equation 6. The diffuser performance of a given geometry of jet pump could then be predicted for a known downstream back pressure.

The results contributing to, and culminating in, Figure 14 cover diffuser cone angles from 7° to 20°, area ratios from 2 to 5.6, and inlet Reynolds numbers from $4.3 \times 10^4$ to $1.3 \times 10^6$ and are therefore considered to be widely applicable. They certainly extend well beyond the optimum diffuser (near 7°) cases and distortion factors quoted by previous researchers. It should be borne in mind, however, that these are CFD predictions.

## References


Cockrell, D. J. and Markland, E. 1963. A review of incompressible diffuser flow. *Aircraft Engineering*, **35**, 286–292

Engineering Sciences Data Unit. 1973. *Performance of Conical Diffusers in Incompressible Flow* (Data Item No. 73024) (Amendments A & B, 1980). E.S.D.U. International Ltd., London

Engineering Sciences Data Unit. 1976. *Introduction to Design and Performance Data for Diffusers* (Data Item No. 76027) (Amendment A, 1990). E.S.D.U. International Ltd., London

Engineering Sciences Data Unit. 1988a. Ejectors and jet pumps: design and performance for compressible air flow (Data Item No. 84029). E.S.D.U. International Ltd., London

Engineering Sciences Data Unit. 1988b. Ejectors and jet pumps: design for compressible gas flow (Data Item No. 88002). E.S.D.U. International Ltd., London

Ferrett, E. F. C., Lampard, D. and Duggins, R. K. 1972. Performance of truncated conical diffusers with compressible flow. *J. Mech. Eng. Sci.*, **14** (6), 382–388

McDonald, A. T. and Fox, R. W. 1966. An experimental investigation of incompressible flow in conical diffusers. *Int. J. Mech. Sci.*, **8**, 125–139

Migay, V. K. 1963. A study of ribbed diffusers. Aeronautical Research Council (UK) (Paper 25382). Trans. from *Teploenergetika*, **10**, 55–59, 1962

Neve, R. S. 1988. The performance and modeling of liquid jet gas pumps. *Int. J. Heat Fluid Flow*, **9** (2), 156–164

Neve, R. S. 1991. Diffuser performance in two-phase jet pumps. *Int. J. Multiphase Flow*, **17** (2), 267–272

Neve, R. S. and Wirasinghe, N. E. A. 1978. Changes in conical diffuser performance by swirl addition. *Aero. Q.*, **24**, 131–143

Owen, I., Abdul-Ghani, A. and Amini, A. M. 1992. Diffusing a homogenized two-phase flow. *Int. J. Multiphase Flow*, **18** (4), 531–540

Patterson, G. N. 1938. Modern diffuser design. *Aircraft Engineering*, **10**, 267–273

Priest, A. J. 1975. Incompressible turbulent flow in pipes and conical diffusers. Ph.D. thesis, University of Salford, UK

Sovran, G. and Klomp, D. 1965. *Experimentally Determined Optimum Geometries for Rectilinear Diffusers With Rectangular, Conical or Annular Cross-Section* (Res. Pub. GMR-511). General Motors Corporation

Sprenger, H. 1959. Experimentelle Untersuchungen an geraden und gekrummten Diffusoren (No. 27). Mitt. Inst. Aerodyn., Zurich (Min. of Av. Trans. TIL/T5134, May 1962)

Stull, F. D. 1975. Flow regimes in two-dimensional ribbed diffusers. *A.S.M.E. J. Fluids Eng.*, **97** (1), 87–96

Tyler, R. A. and Williamson, R. G. 1967. Diffuser performance with distorted inflow. *Proc. I. Mech. E.*, **182** (Pt. 3D), 115–125

Winternitz, F. A. L. and Ramsay, W. J. 1957. Effects of inlet boundary layer on pressure recovery, energy conversion and losses in conical diffusers. *J. R. Ae. S.*, **61**, 116